The chemotherapeutic drug methotrexate selects for antibiotic resistance

Jónína S. Gudmundsdóttir[1*], Elizabeth G. A. Fredheim[1], Catharina I. M. Koumans[2], Joachim Hegstad[1,3], Po-Cheng Tang[4], Dan I. Andersson[4], Ørjan Samuelsen[1,5] and Pål J. Johnsen[1*]

[1]Department of Pharmacy, Faculty of Health Sciences, UiT The Arctic University of Norway, Tromsø, Norway.

[2]Institute of Biology, Leiden University, Leiden, The Netherlands.

[3]Research and Development Division, Department of Microbiology and Infection Control, University Hospital of North Norway, Tromsø, Norway.

[4]Department of Medical Biochemistry and Microbiology, Uppsala University, Uppsala, Sweden.

[5]Norwegian National Advisory Unit on Detection of Antimicrobial Resistance, Department of Microbiology and Infection Control, University Hospital of North Norway, Tromsø, Norway.

*Correspondence to: jonina.gudmundsdottir@uit.no or paal.johnsen@uit.no

Abstract:

Understanding drivers of antibiotic resistance evolution is fundamental for designing optimal treatment strategies and interventions to reduce the spread of antibiotic resistance. Various cytotoxic drugs used in cancer chemotherapy have antibacterial properties, but how bacterial populations are affected by these selective pressures is unknown. Here we test the hypothesis that the widely used cytotoxic drug methotrexate affects the evolution and selection of antibiotic resistance through the same mechanisms as the antibiotic trimethoprim. We show that methotrexate can select for trimethoprim resistance determinants located on the chromosome or a plasmid in clinical strains of *Escherichia coli*. Additionally, methotrexate can co-select for virtually any antibiotic resistance determinant when present together with trimethoprim resistance on a multidrug-resistance clinical plasmid. These selective effects occur at concentrations 40- to >320-fold below the methotrexate minimal inhibitory concentration for *E. coli,* suggesting a selective role of methotrexate chemotherapy for antibiotic resistance in patients that strongly depend on effective antibiotic treatment.

Keywords:

Chemotherapeutic drugs, antibiotic resistance, methotrexate, resistance evolution.

Introduction

Antibiotic resistance is a major risk factor for patients with impaired immunity, such as cancer patients, and often a patient's survival depends on antibiotic treatment to reduce the risk for hospital-acquired infections during chemotherapy (*1, 2*). Several cytotoxic drugs used in cancer chemotherapy are known to both elevate bacterial mutation rates and have antimicrobial properties (*3, 4*). It has been proposed that cancer chemotherapy may drive *de novo* antibiotic resistance evolution through SOS induced mutagenesis (*5*), and some reports have provided

45 support for this hypothesis (*6, 7*). Recently, the effects of non-antibacterial drugs on bacteria typically found in the human gut were thoroughly explored and cytotoxic drugs were reported to cause the most severe alterations of the microbiota (*8*). Taken together, these studies suggest that cytotoxic drugs affect survival of human gut commensals, they may increase the evolvability of bacterial populations, and lead to reduced susceptibility towards drugs used to
50 treat cancer in bacteria. How bacterial populations respond to selective and co-selective pressures exerted by individual cytotoxic drugs and the implications for antibiotic resistance evolution is unknown. There is an urgent need to understand these potential collateral effects of cancer chemotherapy to ensure effective antibiotic treatment for a large group of immunocompromised patients. Moreover, cytotoxic drugs may constitute a previously
55 unrecognized target for intervention to limit the selection and spread of antibiotic resistance. Here we explored how selective and co-selective pressures exerted by the cytotoxic drug methotrexate (MTX) affect the enrichment and evolution of antibiotic resistance determinants.

MTX, the first effective chemotherapeutic (*9*), is structurally similar to the antibiotic trimethoprim (TMP) and the potential drug interactions and toxic effects associated with
60 combination therapy are well known (*10*). Both drugs act through inhibiting the dihydrofolate reductase enzyme in bacteria and eukaryotic cells (*11*) and are commonly used to treat a variety of diseases. TMP in combination with sulfamethoxazole is among the most frequently used antibiotics in the treatment of urinary tract infections and is recommended as first line treatment internationally (*12*). MTX is widely used in treatments including but not limited to; cancer of
65 the breast, skin, head, neck, and lung as well as many inflammatory diseases, such as rheumatoid arthritis (*13*), making it one of the most commonly prescribed drugs in the USA (*14*).

Here, we tested the hypotheses that MTX directly selects for bacterial TMP resistance (TMP^R) and co-selects for other antibiotic resistance determinants when co-residing on a

70 mobile genetic element. We exposed a clinical *Escherichia coli* strain to a wide concentration range of MTX and observed that MTX selects for mutations identical to those that occur when TMP was used as selective agent. We determined the minimum selective concentrations (MSCs) of MTX for chromosomal and plasmid mediated TMP^R determinants and show that positive selection occurs at concentrations 40- and >320-fold below the minimum inhibitory
75 concentrations (MICs), respectively.

Results

Methotrexate selects for pre-existing trimethoprim resistance determinants

We determined the MICs of MTX in clinical and laboratory strains of *E. coli* (Table S1), the
80 most frequently isolated bacterial species from urinary tract and blood stream infections (*15*). Initial experiments revealed variable, but consistently high MTX MICs (Table S2). This is consistent with previous reports indicating that *E. coli* displays reduced susceptibility towards MTX due to AcrAB-TolC mediated efflux (*8, 16*). We also observed that the MTX MIC was dependent on the presence of TMP resistance determinants. All isolates with a functional TMP
85 resistance determinant and increased TMP MIC showed consistently higher MTX MICs (>32 mg/mL) than TMP susceptible isolates (4-32 mg/mL) indicating possible co-selective abilities of the two drugs.

Antibiotic resistance selection and co-selection have traditionally been assumed to occur between the MICs of susceptible and resistant isolates (known as the selective window)
90 within a bacterial population (*17*). However, several reports unequivocally show that antibiotic resistance selection and co-selection can occur at concentrations several hundredfold below the MIC of the susceptible isolate (known as sub-MIC) (*17-19*). To test how sub-MICs of MTX affect bacterial fitness, we measured exponential growth rates for two pairs of clinical isogenic trimethoprim resistant and susceptible (TMP^S) *E. coli* across a wide MTX concentration span.

95 One pair with TMP^R located on the chromosome (two mutations associated with *folA*) and one pair with TMP^R (*dfrA*) located on the multidrug-resistance (MDR) plasmid pG06-VIM-1 (*20, 21*). TMP^S strains displayed sharply declining growth rates between 1 and 2 mg/mL of MTX, whereas the TMP^R strains remained unaffected (Figure S1). These results suggest a selective benefit during MTX exposure for TMP^R strains at concentrations below the observed MTX

100 MIC of the TMP^S clinical isolates.

The MSC describes pharmacodynamically the lowest concentration where selection for resistance occurs (*17*). To determine the MSC for MTX, we constructed a pair of *E. coli* MG1655 strains with yellow (*sYFP2*) and blue (*mTagBFP2*) fluorescent proteins to enable accurate separation between the two in mixed populations. In these backgrounds, we introduced

105 chromosomal TMP^R mutations (*folA*) using genome engineering (*22*) and moved the pG06-VIM-1 plasmid into the fluorescently-tagged strains. The isogenic TMP^R and TMP^S strain pairs were competed head-to-head by serial passage for 30 generations and the ratio of TMP^R:TMP^S was determined over time using flow cytometry. From this data the MSC was estimated (Tables S3-S5) (*17*). *E. coli* with chromosomal *folA* mutations had an MSC of 200 μg/mL (1/40 of the

110 MIC of MTX) whereas those harboring the plasmid were close to the detection limit of the assay (*17*) and we conservatively estimated the MSC to be <25 μg/mL (less than 1/320 of the MIC of MTX) (Figure 1). Taken together, our data strongly suggest that selection for TMP^R occurs at MTX concentrations far below the estimated MTX MIC.

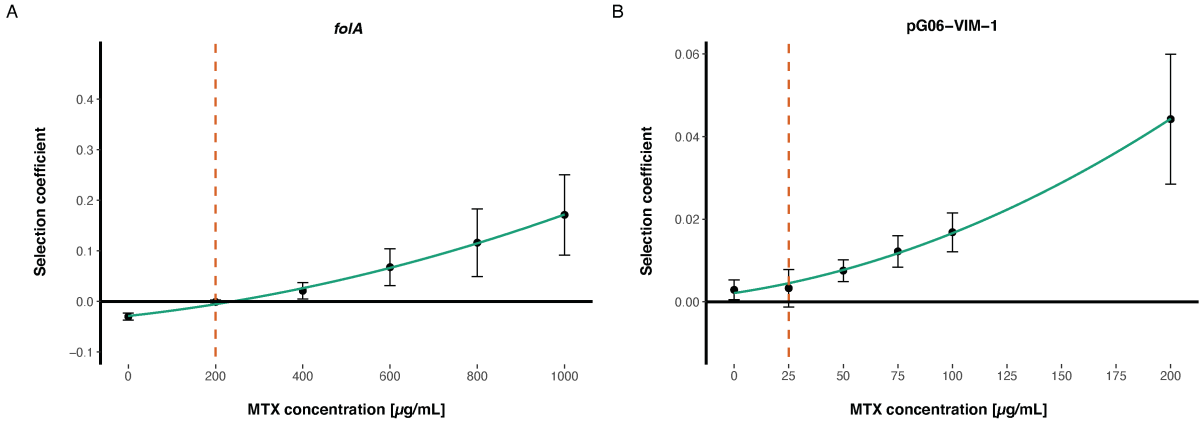

Figure 1: Selection coefficients as functions of MTX concentrations from competition experiments between TMP^R and TMP^S isogenic strains. The MSC is defined as the concentration where the selection coefficient equals zero. The MSC of *E. coli* MG1655 harboring **(A)** two chromosomal *folA* mutations (MP18-04 and MP18-07) is set to 200 µg/mL, and **(B)** the MDR pG06-VIM-1 encoding *dfrA12* (MP18-05 and MP18-08) is conservatively set below 25 µg/mL. Dashed lines represent the set MSC, bullets the average selection coefficients and error bars the standard deviations.

Methotrexate resistance determinants invade when rare in *E. coli* populations

Exploring MTX-selective dynamics further, we asked if TMP^R determinants could invade the population at lower initial densities to exclude potential bias from the 1:1 ratio in the competition experiments. We started competition experiments from frequencies as low as 10^{-4} of the TMP^R strains, at concentrations slightly above the estimated MSC of MTX (400 µg/mL for *folA* mediated resistance and 75 µg/mL for pG06-VIM-1 mediated resistance) and followed the change in ratios over 30 generations of growth (Figure 2). Both chromosomal and plasmid mediated TMP^R determinants were able to invade, even when initially rare in their respective populations, strongly suggesting that the MTX-selective effects are independent on initial frequencies of resistant and susceptible strains during competition experiments.

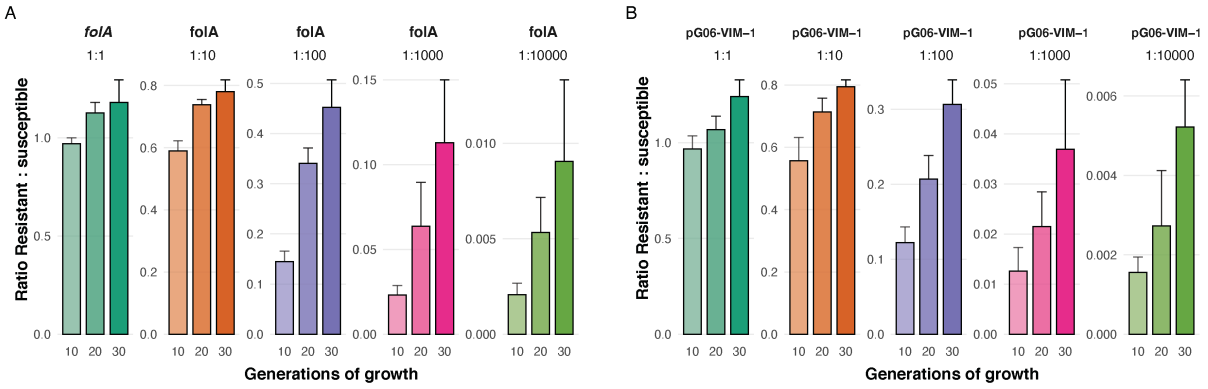

Figure 2: Competition experiments during MXT exposure at different initial frequencies of TMP^{R} strains. The change in TMP^{R}:TMP^{S} ratios over 30 generations of growth at MTX concentrations slightly above the MSCs where *E. coli* MG1655 harbors **(A)** two *folA* mutations (MP18-07), and **(B)** the pG06-VIM-1 plasmid (MP18-08) were competed against a differently tagged, isogenic susceptible strain (DA56507) at 1:1, 1:10^{-2}, 1:10^{-3} and 1:10^{-4} starting ratios. Error bars represent the standard deviation of the average ratio.

Methotrexate co-selects for resistance determinants on a multi drug resistance plasmid

Both phenotypic and genotypic stability was recently demonstrated for the pG06-VIM-1 plasmid in *E. coli,* when serially passaged in the absence of any selective pressure over 300 generations (*21*). To ensure the stability of pG06-VIM-1 in our strains competing in the presence of MTX, three independent linages of K56-75 harboring the plasmid (MP05-31) were serially passaged by 100-fold dilution in 1 mL batch cultures with 400 µg/mL MTX supplemented for 50 generations. The lineages were then plated non-selectively on MHII agar and 100 colonies from each lineage tested for reduced susceptibility towards ampicillin, TMP, streptomycin and spectinomycin. The results revealed complete phenotypic stability across all three lineages, confirming not only plasmid stability but also MTX mediated co-selection of MDR.

To verify that the TMP^R as well as methotrexate resistance (MTX^R) observed in strains
155 harboring the pG06-VIM-1 MDR plasmid (Table S2) is indeed mediated by the *dfrA* genes found on the plasmid, both *dfrA1* and *dfrA12* were isolated from the plasmid and cloned onto an expression vector and the effects of the individual genes measured. Of the two genes it was only the *dfrA12* gene that was shown to give the same resistance pattern for TMP as well as MTX as the pG06-VIM-1 plasmid, and the lack of detectable phenotype for *dfrA1* (MP18-11)
160 is likely due to a start codon frameshift mutation (*21*).

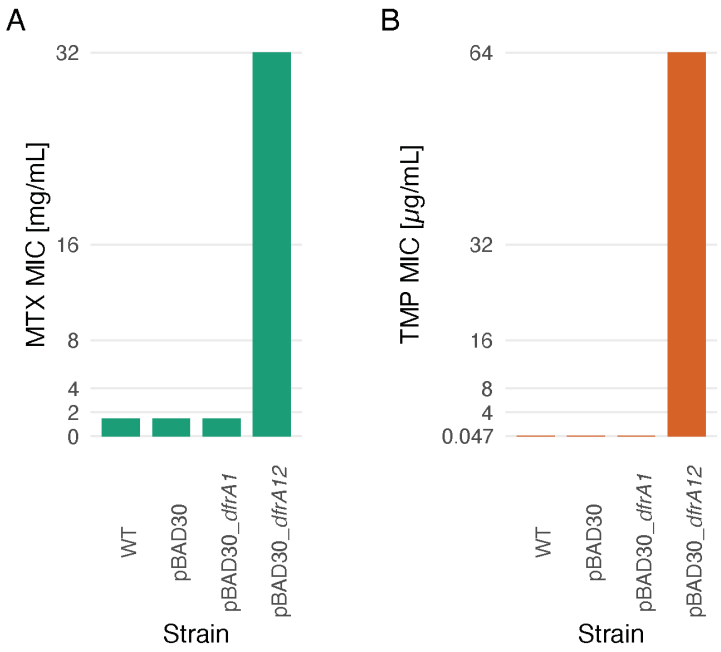

Figure 3: MIC measurements of *dfrA1* and *dfrA12* show that MTX and TMP resistance conferred by the pG06-VIM-1 plasmid is caused by the *dfrA12* gene. The MTX **(A)** and
165 TMP **(B)** MIC for the WT *E. coli* DH5α (MP18-09) compared to the strain harboring the empty pBAD30 (MP18-10) expression vector as well as strains with pBAD30 with different *dfrA* genes expressed under the inducible expression control by the pBAD promotor (MP18-11 and MP18-12). The detection limit of the assay is 64 µg/mL for TMP and 32 mg/mL for MTX. For both drugs, the MIC of *E. coli* DH5α conferring pBAD30 expressing *dfrA*12 (MP18-12)
170 exceeded the detection limit.

Methotrexate selects for *de novo* trimethoprim resistance

We further examined whether exposure to MTX could lead to *de novo* TMP^R evolution. We selected spontaneous mutants from overnight cultures with and without exposure to MTX, plated on selective agar at high MTX concentrations and tested for TMP cross-resistance
175 (Figure S2, Table S6). *E. coli* K56-2 isolated at 16 and 32 mg/mL MTX (MP18-17 to MP18-28) displayed increased MICs of TMP close to or above the clinical breakpoint (*23*), clearly demonstrating selection for TMP^R by MTX. DNA sequencing of the resistant isolates revealed two different mutations in the *folA* promoter, previously reported to result in TMP^R (*24*), as well as a single mutation in the *marR* gene (Table S6-S11).

180 Finally, we asked if exposure to sub-MICs of MTX close to the estimated MSCs would select for *de novo* TMP^R mutations in a susceptible *E. coli* population. Starting from 1,000 cells to minimize the probability of pre-existing mutants, we grew 10 independent lineages of the *E. coli* K56-2 strain at 400 μg/mL MTX for 500 generations. The frequency of TMP^R was determined every 50 generations. TMP^R ascended in frequency in 2/10 lineages at different
185 rates and time-points during the first 250 generations before they were outcompeted by a different set of mutants with reduced susceptibility to MTX and no cross-resistance to TMP (Figure 4, Table S12). These experiments show that MTX exposure can select for *de novo* TMP^R, both at high and sub-MIC concentrations.

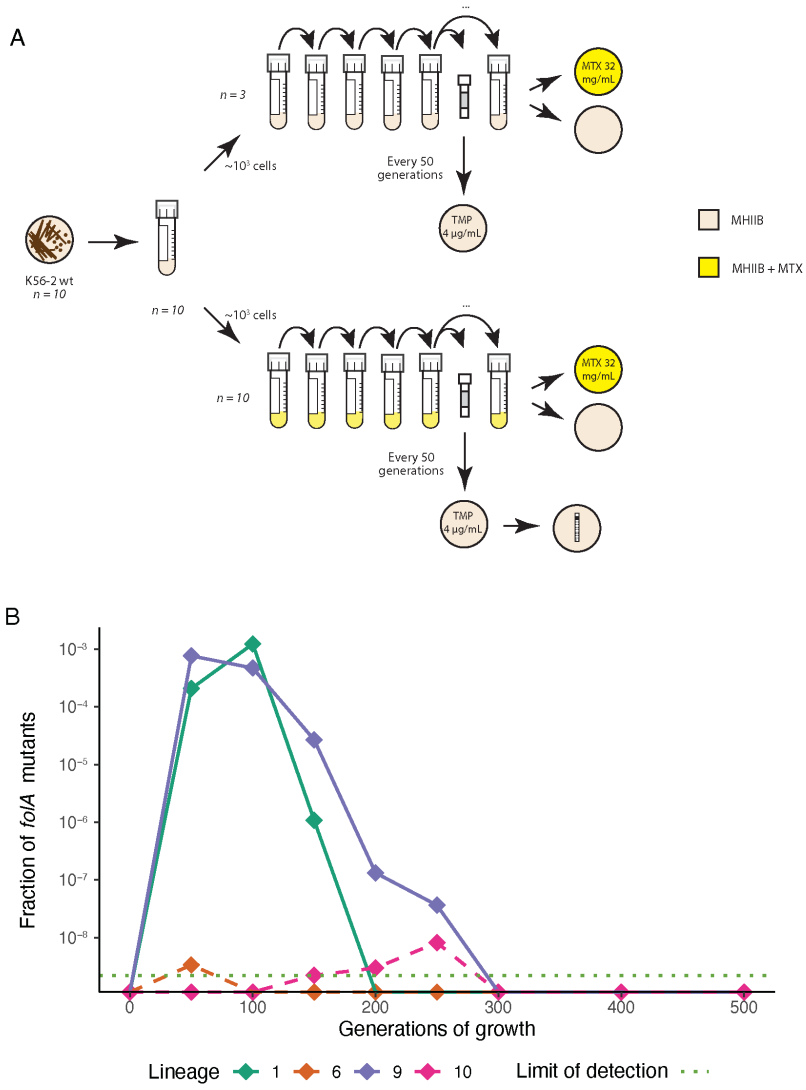

Figure 4: Evolution of TMP^R during MTX exposure for 500 generations. (A) Sub-MIC evolution experimental set-up. Ten biological replicates of K56-2 (MP06-01) were evolved for ~500 generations with 400 µg/mL MTX and three without drug. All lineages were screened for TMP^R every 50 generations. After 500 generations all end-point populations were plated on 32 mg/mL MTX. All populations were able to grow at 32 mg/mL MTX, but not a single clone isolated conferred TMP^R, strongly suggesting that reduced susceptibility to MTX with no cross-resistance to TMP evolved in the endpoint populations. **(B)** Fractions of TMP^R *folA* mutants isolated every 50 generations from the lineages where these were detected. The detection limit of the assay was ~2x10^{-9}. Solid lines represent the two lineages where TMP^R emerged and ascended in frequency whereas dotted lines indicate spontaneous mutants.

Pharmacokinetic approximations

To assess pharmacokinetic relevance, we attempted to estimate the MTX concentration range likely to be found in the intestine of patients undergoing MTX treatment. Limited information is available on gut MTX concentrations during cancer treatment, as pointed out by others (*8*).
205 Pharmacokinetic data reveal that up to 90% of administered MTX is renally excreted (*25*) and we assume that the remaining ~10% of the dose constitutes the upper limit of the concentration range present in the human intestine. The lower limit is set to 2% of the dose based on the mean ^{3}H labelled MTX concentrations measured in stool samples from nine patients receiving MTX intravenously (*26*). From this, we set a 24 hour transition time in a total volume of 0.6 L (*8*)
210 and calculated the dose (d) required to achieve MSC in the human intestine from:

$$\frac{d}{0.6L}\ x\ (0.1\ or\ 0{,}02) = MSC$$

Estimated doses needed to reach intestinal MSCs assuming 2% and 10% fecal MTX fecal concentrations were from 0.15g to 0.75g for plasmid-mediated TMP^{R} and from 1.2g to 6g for chromosomal *folA* mutations. Thus, assuming close to 2m^{2} body surface in grown-up patients
215 (*27*) estimates of MSC for plasmid-mediated TMP^{R} translates to dosing regimens from 75-375 mg/m^{2} and from 0.6-3 g/m^{2} for the chromosomal *folA* mutations. These approximations indicate that our MSC estimates are relevant for patients receiving high dose MTX treatment (1-12 g/m^{2}) (*28*).

220 **Discussion**

Here we show that exposure to the cytotoxic drug MTX affects selection and evolution of TMP^{R} determinants at clinically relevant concentrations. Notably, MTX can mediate selection of any antibiotic resistance determinant when TMP^{R} is co-localized on a mobile genetic element across a wide concentration gradient. Arguably, this potentially important side-effect of MTX
225 treatment has been previously unrecognized, as studies on the effects of non-antibiotic drugs,

including MTX, have either focused on bacterial growth inhibition or used drug concentrations around the MIC (*8, 29-31*), with a few exceptions (*18, 32*). Using the approaches outlined here, including high resolution mixed culture competition experiments, allow determination of the true MTX selective window ranging from the MSC to the MIC (*17*). This is particularly relevant
230 for non-antibiotics for which bacteria display reduced susceptibility. In *E. coli,* MTX is a substrate for the AcrAB-TolC efflux pump (*16*) and selective effects as those demonstrated here would not have been detected in classical susceptibility and/or growth assays in bacterial mono-cultures. This was recently supported in an *E. coli* chemical genetic screen where clear growth inhibitory effects of MTX, as well as for a range of other non-antibiotics, were only
235 demonstrated in a *tolC* knock-out mutant (*8*).

Given that many cytotoxic drugs are structurally similar to antibiotics (e.g. doxorubicin/tetracyclines), or target similar key processes as the major antibiotic groups (e.g. DNA/protein synthesis) it is possible that cancer chemotherapy may lead to increased levels of antibiotic resistance in a vulnerable patient group that very often rely on efficient antibiotic
240 treatment for survival. To acquire a deeper understanding of the evolutionary potential of novel, non-antibiotic drivers of antibiotic resistance the approaches presented here are essential. These approaches need to be combined with an improved understanding of the intestinal pharmacokinetics of MTX and other cytotoxic drugs, possible effects of co-administered drugs such as leucovorin mediated MTX rescue (*33*), and their interactions with the human
245 microbiome. Such knowledge could allow identification of antibiotic + non-antibiotic drug combinations that should be avoided to preempt resistance evolution.

Recent studies have showed that non-antibiotics can increase mutation rates (*6, 7*) and promote horizontal gene transfer (*32, 34*). Taken together with the data presented here it is clear that non-antibiotic drugs have the potential to affect the evolution, selection, and spread of
250 antibiotic resistance determinants. It is also clear that without a better understanding of these

potential drivers of antibiotic resistance, interventions including those targeting human consumption of antibiotics may be negatively affected.

Materials and methods

255 Bacterial strains and growth conditions

Bacterial strains used in this study and their assigned reference numbers are listed in Table S1. Most strain constructs were derived from the *E. coli* K-12 strain MG1655 (DA4201/DA5438), or for cloning purposes from *E. coli* DH5α (MP18-09). Two isogenic pairs of clinical *E. coli* strains, where one strain is TMP^S and the other is TMP^R, were used for fitness measurements.
260 In the first pair, TMP^R in *E. coli* K56-2 (MP06-01) is caused by one intragenic point mutation T>A (W30R) in the *folA* gene, and one in its promotor region (P_{folA}, C>T 58 base pairs (bp) upstream of the gene) (*20, 35*) (MP06-05). In the second pair, *E. coli* K56-75 (MP06-41) harbored the pG06-VIM-1 MDR plasmid. This plasmid encodes, amongst other antibiotic resistance genes, two different *dfrA* genes (*dfrA1* and *dfrA12*) as putative TMP^R determinants
265 as well as carbapenem resistance (bla_{VIM-1}) (*21*) (MP05-31). All incubations of liquid cultures were performed with orbital shaking (225 rpm) at 37°C, unless otherwise specified. Cultures were grown in Miller Difco Luria-Bertani (LB) broth (Becton, Dickinson and Co.) or SOC (20 g/L tryptone (Oxoid), 5 g/L yeast extract (Oxoid), 0.5 g/L NaCl (VWR), 0.25 mM KCl (Sigma-Aldrich), 10 mM $MgCl_2$ (Sigma-Aldrich), 4 g/L glucose (Sigma-Aldrich). When required,
270 medium was supplemented with 1.5% (w/v) agar (Sigma-Aldrich) to form solid medium. For assays involving either antibiotics or cytostatics, the bacteria were grown in cation adjusted Mueller-Hinton II Broth (MHIIB, Becton, Dickinson and Co.), supplemented with the relevant drug. For assays done on strains harboring the pBAD30 expression vector, cultures were supplemented with 0.2% (w/v) arabinose (Sigma-Aldrich) for induction. Generalized
275 transduction using the P1*vir (36)* were used to move chromosomal markers between strains. For selection against cells expressing *sacB*, sucrose selection plates (5 g yeast extract (Oxoid), 10 g Tryptone (Oxoid), and 1 mM NaOH per liter (VWR), 5 % (w/v) sucrose (Sigma-Aldrich)) were used (*29*). When appropriate, media were supplemented with: 12.5 mg/L chloramphenicol

(Sigma-Aldrich), 7.5 mg/L tetracycline (Sigma-Aldrich). For long-term storage, strains and
280 populations were mixed with glycerol at a final concentration of 20 % (v/v) and frozen at −80 °C.

Strain Constructions

A promoter-levansucrase-chloramphenicol resistance-promoter cassette (P_{CP25}-*sacB-cat*-
285 P_{J23101}) was first constructed by amplifying the *sacB-cat*-P_{J23101} cassette (GenBank accession number KM018298) by using primers with 40 bp sequence homologous to each end of the *insKJ* and partially *mokA* genes in the IS*150* region on the *E. coli* MG1655 chromosome (Table S13). The construct was introduced onto the chromosome by λ Red recombineering (*37, 38*) in a strain carrying the pSIM5 plasmid (*39*) with tetracycline as the antibiotic selection marker
290 (pSIM5-*tet*, DA45134). Chloramphenicol resistance was used to select for the inserted construct.

Fluorescent protein encoding: *bfp* (*cat*-PJ23101-*mtagBFP2*, blue; (*18*) GenBank accession number KM018299), *yfp* (*cat*-PJ23101-*SYFP2*, yellow; (*18*); GenBank accession number KM018300) were PCR amplified from previous strains (*18*). Both amplifications were
295 carried out using Phusion High-Fidelity DNA Polymerase (Thermo Scientific). Reaction primers were designed with one of the 40 bp homology to the disrupted IS*150* locus whilst the other retained the P_{CP25} promoter (Table S13). Reaction products were purified using the GeneJet Purification Kit (Thermo Scientific) and introduced onto the chromosome by λ Red recombineering by counter-selection on sucrose agar medium. This resulted in [P_{CP25}-*sYFP2*]
300 and [P_{CP25}-*mtagBFP2*] constructs.

Dup-In methodology of the IS*150* locus was then carried out on all previous constructs (*40*) using the *sacB-cat*-P_{J23101} cassette (GenBank accession number KM018298) and chloramphenicol resistance as the antibiotic selection. P1*vir* lysates for both fluorescent

markers were prepared and transduced into a common background (DA4201) by generalized
305 transduction and segregation of Dup-Ins. Briefly, transduced colonies were picked from plates first with chloramphenicol resistance to transfer the Dup-In with the IS*150* locus, then single colonies were patched on sucrose plates for loss of the *sacB-cat*-P_{J23101} cassette but retaining of the IS*150* locus. For screening of the final strains constructed and generation of templates for Sanger sequencing, DreamTaq PCR Master Mix (Thermo Scientific) was used.

310 The fluorescently tagged strains were then further engineered to obtain TMP^R derivatives. Two point mutations associated with *folA* (the first a non-synonymous point mutation in the *folA* gene, W30R, and the second a point mutation 58 bp upstream of the *folA* gene within the promotor region, C>T) were carefully introduced onto the chromosome of the strains using a double MAGE cycle with the pORTMAGE-2 plasmid as described by its
315 constructors (*22*). The carbapenemase-encoding plasmid pG06-VIM-1 (encoding two *dfrA* genes, *dfrA1* and *dfrA12(21)*), was transformed into the fluorescently tagged strains using room temperature electroporation (*41*).

To verify the role of *dfrA* genes in both TMP^R as well as methotrexate resistance (MTX^R), both *dfrA1* and *dfrA12* were PCR amplified using Phusion High-Fidelity DNA
320 Polymerase (New England BioLabs® Inc.), purified using QIAquick® PCR Purification Kit (QIAGEN), phosphorylated using T4 Polynucleotide Kinase (Thermo Scientific) and cloned using T4 DNA Ligase (Thermo Scientific) into the pBAD30 vector at the *Sma*I site. Thus, the expression of the *dfrA* genes was under the tight inducible control by the P_{BAD} promotor when in the presence of arabinose (*42*). The purified ligation reactions were transformed into
325 electrocompetent DH5-α cells with electroporation and clones carrying the vector-born *dfrA* genes isolated.

Susceptibility testing

330 Due to the bacteriostatic activities of MTX and a lack of a gold standard for MTX microbiological assays we define the MIC of MTX in this study as the 90% inhibitory level (IC_{90}). This allows for a high resolution and has previously been used as a proxy for the MIC (*43*). The IC_{90} values for TMP were determined as described previously (*20*). The IC_{90} values for MXT, using Methotrexate Teva/Ebetrex 100 mg/mL (Pharmachemie B.V./Ebewe Pharma

335 Ges.m.b.H Nfg.KG), were determined using the same protocol with small changes. Briefly, 96-well plates were incubated at 300 rpm (3 mm stroke) for 18 h at 37°C before the OD_{600} was measured using an Epoch 2 Microplate Spectrophotometer (BioTek Instruments, Inc.)/VersaMax™ ELISA Microplate (Molecular Devices®). Internal controls were included on all plates. Percent inhibition was calculated as previously described (*44*). All measurements

340 were done using at least three biological replicates where the MIC was set as the most read (modal) value on a two-fold scale of replicates that met quality control standards (Table S2). For characterization of TMP^R mutants isolated from the MTX sub-MIC evolution, TMP MIC was determined by gradient diffusion strips following the manufacturer's guidelines (Liofilchem). Measurements were done using two to four biological replicates, where the MIC

345 was set as the most read (modal) value (Table S12).

Growth rate measurements

Growth rates were determined using a BioscreenC MBR reader (Oy Growth Curves Ab, Ltd). A minimum of five independent overnight cultures were diluted to ~5 x 10^6 CFU/mL in MHIIB.

350 Two 300 µL aliquots of each dilution were transferred into sterile Honeycomb plates (Oy Growth Curves Ab, Ltd). The samples were grown at 37°C with continuous shaking for 18 h and OD_{600} values were measured every 4 min. The growth curves from the Bioscreen measurements were analyzed and growth rate calculations done using the statistical software R

(*45*) and the Bioscreen Analysis Tool BAT 2.1 (*46*). Calculations were based on OD_{600} values
355 between 0.02 and 0.1, where growth was observed to be exponential. Relative growth rates were calculated by dividing the generation time of the sample strain by the generation time of the parental strain.

Competition experiments

360 Competition experiments were performed using the fluorescently tagged strain pairs, both for *folA* and pG06-VIM-1 mediated TMP^R. A susceptible strain tagged with either *yfp* or *bfp* was mixed at 1:1 ratio with the constructed TMP^R strains harboring the disparate fluorescence marker to initiate a head-to-head competition, at different MTX concentrations. Six independent cultures (~5 x 10^9 CFU/mL) of each strain were used to start 12 competitions, i.e.
365 six biological replicates for each color arrangement in a dye-swap set-up. Every 24 h for three to four days the competing strains were passaged 1:1,000 into fresh medium and the mutant to wild type (WT) ratio measured by counting 10^5 cells using a fluorescence-activated cell sorter (BD FACS Aria III). For safety reasons, all cultures were washed in fresh drug-free MHIIB in order to remove remains of cytostatic drugs from the cultures before being moved over to the
370 cell sorter for analysis. Cells were gently pelleted at 5000 rcf at 4°C for 5 min before removal of the supernatant containing drug, followed by resuspension of the cells in fresh MHIIB.

Selection coefficients were calculated according to the regression model $s=[\ln R(t)/R(0)]/t$, as previously described (*47*), where R is the mutant to WT ratio and t is the time measured in generations of growth (Tables S3-S5). The minimum selective concentration
375 (MSC) is defined as the concentration where the selection coefficient equals zero (where the regression line crosses the x-axis) (*17*).

In a similar way, six individual cultures of a susceptible *yfp* strain was competed against the *bfp* resistant strains in 1:1, 1:10, 1:10^2, 1:10^3 and 1:10^4 starting ratios of TMP^R:TMP^S strains

at concentrations slightly above the estimated MSCs (400 μg/mL for *folA* mutant, 75 μg/mL
380 for p06-VIM-1).

Selective plating on high concentrations of MTX

Single MTX resistant mutants of K56-2 (MP06-01) were selected at lethal MTX concentrations. Dense overnight cultures grown in drug-free LB was concentrated 10×, and 100
385 μL spread on LB agar plates supplemented with 4, 8 and 16 mg/mL MTX. Due to the slow growth of mutants, the plates were incubated between 48 to 96 h before mutants were purified on non-selective plates. Additionally, an overnight culture grown in LB containing MTX at the estimated MIC concentration was concentrated 10× and 100 μL spread on LB agar plates with and without MTX 32 mg/mL. After 48 h incubation, mutants were purified on non-selective
390 plates. The MTX and TMP MICs for all mutants isolated were determined as previously described by IC_{90} testing (*20*) and the *folA* gene, its promotor area and the *marR* gene sequenced with Sanger sequencing and analyzed using the CLC Main Workbench (Qiagen) (Table S6).

Laboratory evolution at sub-MICs of MTX

395 To examine the effect of MTX presence on TMP^R evolution, strain K56-2 (MP06-01) was serially passaged in liquid cultures with MTX supplemented at concentration slightly above the estimated MSC. Initially, 10 independent overnight cultures were started from independent colonies on separate agar plates. From the original overnight cultures, ~10^3 cells were used to start ten independent lineages in 1 mL MHIIB containing 400 μg/mL MTX (lineages 1-10).
400 Every 12 h for 25 days, the lineages were serially passaged by 1,000-fold dilution in 1 mL batch cultures, allowing for ~500 generations of growth. Every ~50 generations the populations were frozen down at –80°C for downstream analysis. In parallel, three independent control lineages were simultaneously sampled for TMP resistance under the same experimental conditions

except for MTX exposure (lineages 11-13). All end-point populations were plated on MHII
405 agar plates containing 32 mg/mL MTX after ~500 generations of growth. From lineages 1-10, 20 colonies were isolated from each lineage and tested for TMP^R. Of those, none displayed increased resistance towards TMP compared to the parental strain. To examine possible evolution of cross-resistance towards TMP in the laboratory evolution experiment described above, all 13 frozen populations from every 50 generations were gently thawed on ice and
410 dilution series plated on both MHII agar plates containing TMP 4 μg/mL as well as on MHII agar without any drug, and frequencies of TMP resistant mutants calculated. From each plate where mutants grew, up to 5 colonies were randomly isolated, their susceptibility towards TMP measured, and the *folA* gene and its promotor area sequenced with Sanger sequencing and analyzed using the CLC Main Workbench (Qiagen) (Table S12). No MTX^R or TMP^R colonies
415 were isolated from the lineages grown without drug presence (lineage 11-13). This was done to control for the emergence and selection of spontaneous mutants in a drug-free environment.

Whole genome sequencing

To investigate the possibility of additional genetic changes, other than the TMP^R determinants
420 shown to be associated with reduced susceptibility towards MTX, during MTX selection, five isolates from the lethal selection were chosen (MP18-13, MP18-17, MP18-20, MP18-26 and MP18-28) based on their different susceptibility profiles and subjected to whole genome sequencing (WGS). Bacteria were grown overnight and genomic DNA prepared using GenElute™ Bacterial Genomic DNA Kit (Sigma-Aldrich) following the protocol provided by
425 manufacturer with slight adaptions. In brief, 1.5 mL of dense culture (OD_{600}: 0.8-1.0) was pelleted by centrifugation at 13,000 rpm, culture medium removed and the pellet resuspended in 200 μL lysozyme solution (100 mg/mL) and incubated for 30 min at 37°C before 20 μL of RNase A solution was added and incubated for 2 min at room temperature. Following, 20 μL

of Proteinase K (20 mg/mL) and 200 μL of Lysis solution C were added to the mixture and
430 incubated at 55°C for 10 min after being thoroughly vortexed. To each pre-assembled GenElute Miniprep Binding Column, 500 μL of the Column Preparation Solution were added, 200 μL of ethanol (95-100 %) was then added to the lysate and thoroughly mixed before the lysate was carefully loaded onto the binding column, centrifuged at 13,000 rpm for 1 min and then washed 2× with 500 μL of Wash Solution. Genomic DNA was eluted in 100 μL of 10 mM Tris-base
435 and purity and concentration determined using NanoDrop One (Thermo Scientific) and Qubit (Thermo Scientific) respectively. Next-generation sequencing libraries were prepared from the bacterial genomic DNA samples and sequenced on an Illumina NovaSeq with a 2 × 150 bp configuration (GENEWIZ). Average whole genome coverage per sample was approximately 700. Analysis of the fastq files obtained from Illumnia sequencing was performed using an in-
440 house bioinformatic pipeline (Table S14) to compare the mutant sequences to the previously published WT strain (available at NCBI, BioSample SAMN08095529). Where single-nucleotide polymorphisms (SNPs) were identified with a coverage below 100 the evidence was considered insufficient and the SNPs were removed from the analysis. Raw sequence reads were deposited under BioProject PRJNA677979.

445

Acknowledgments: We thank: Fredrik Sund, MD at The University Hospital North Norway for valuable input on medical aspects of MTX. Ass. Prof. Daniel Rozen, Leiden University for valuable discussions. Prof. Natasa Skalko-Basnet and Ass. Prof. Ann Mari Holsæter, UiT The Arctic University of Norway, for training in handling of cytostatic drugs. **Funding**: PJJ was
450 supported by a joint grant from UiT The Arctic University of Norway and the Northern Norway Regional Health Authorities (A23270). DIA was supported by the Swedish Research Council (grant 2017-01527).

Author contributions: The study was designed by JSG, EGAF, ØS and PJJ. Strain constructions were done by PT and JSG. Experiments were conducted by JSG, EGAF and CIMK. WGS was done using a bioinformatic pipeline designed by JH. Formal data analysis and data visualization was done by JSG. The first draft of the manuscript was written by JSG and revised by PJJ. All authors revised subsequent version and provided constructive feedback on the manuscript. Funding acquisition and resources were provided by PJJ and DIA.

Competing Interests: The authors declare no competing interests. **Data availability:** WGS data are available at NCBI (BioProject PRJNA677979).

References:

1. A. Teillant, S. Gandra, D. Barter, D. J. Morgan, R. Laxminarayan, Potential burden of antibiotic resistance on surgery and cancer chemotherapy antibiotic prophylaxis in the USA: a literature review and modelling study. *The Lancet Infectious Diseases* **15**, 1429-1437 (2015). https://doi.org/10.1016/S1473-3099(15)00270-4.
2. P. A. Danai, M. Moss, D. M. Mannino, G. S. Martin, The Epidemiology of Sepsis in Patients With Malignancy. *Chest* **129**, 1432-1440 (2006). https://doi.org/10.1378/chest.129.6.1432.
3. S.-i. Nakamura, Y. Oda, T. Shimada, I. Oki, K. Sugimoto, SOS-inducing activity of chemical carcinogens and mutagens in *Salmonella typhimurium* TA1535/pSK1002: examination with 151 chemicals. *Mutation Research Letters* **192**, 239-246 (1987). https://doi.org/10.1016/0165-7992(87)90063-7.
4. G. E. Foley *et al.*, A comparative study of the use of microorganisms in the screening of potential antitumor agents. *Annals of the New York Academy of Sciences* **76**, 413-438; discussion 438-441 (1958). https://doi.org/10.1111/j.1749-6632.1958.tb54862.x.
5. L. E. Papanicolas, D. L. Gordon, S. L. Wesselingh, G. B. Rogers, Not Just Antibiotics: Is Cancer Chemotherapy Driving Antimicrobial Resistance? *Trends in Microbiology* **26**, 393-400 (2018). https://doi.org/10.1016/j.tim.2017.10.009.
6. A. Meunier *et al.*, Enhanced emergence of antibiotic-resistant pathogenic bacteria after *in vitro* induction with cancer chemotherapy drugs. *Journal of Antimicrobial Chemotherapy* **74**, 1572-1577 (2019). https://doi.org/10.1093/jac/dkz070.
7. C. A. Hobson *et al.*, Impact of anticancer chemotherapy on the extension of beta-lactamase spectrum: an example with KPC-type carbapenemase activity towards ceftazidime-avibactam. *Scientific Reports* **10**, 589 (2020). https://doi.org/10.1038/s41598-020-57505-w.
8. L. Maier *et al.*, Extensive impact of non-antibiotic drugs on human gut bacteria. *Nature* **555**, 623-628 (2018). https://doi.org/10.1038/nature25979.

9. S. Farber, Temporary remissionsin acute leukemiain children producedby folic acid antagonist…aminopterin. *CA: A Cancer Journal for Clinicians* **24**, 297-205 (1974). https://doi.org/10.3322/canjclin.24.5.297.
10. J. Bourré-Tessier, B. Haraoui, Methotrexate drug interactions in the treatment of rheumatoid arthritis: a systematic review. *The Journal of Rheumatology* **37**, 1416-1421 (2010). https://doi.org/10.3899/jrheum.090153.
11. R. V. Mauldin, M. J. Carroll, A. L. Lee, Dynamic dysfunction in dihydrofolate reductase results from antifolate drug binding: modulation of dynamics within a structural state. *Structure* **17**, 386-394 (2009). https://doi.org/10.1016/j.str.2009.01.005.
12. P. Bergstrom, S. Holm, K. Grankvist, R. Henriksson, Interaction between antibiotics and antineoplastic drugs on antibacterial activity in vitro: Estramustine phosphate sensitizes pneumococci to amikacin. *International Journal of Oncology* **4**, 435-439 (1994). https://doi.org/10.3892/ijo.4.2.435.
13. J. Jolivet, K. H. Cowan, G. A. Curt, N. J. Clendeninn, B. A. Chabner, The Pharmacology and Clinical Use of Methotrexate. *New England Journal of Medicine* **309**, 1094-1104 (1983). https://doi.org/10.1056/nejm198311033091805.
14. S. P. Kane, "ClinCalc DrugStats Database, Version 20.2," (ClinCalc LLC, 2020; https://clincalc.com/DrugStats).
15. M. J. Struelens, O. Denis, H. Rodriguez-Villalobos, Microbiology of nosocomial infections: progress and challenges. *Microbes and Infection* **6**, 1043-1048 (2004). https://doi.org/10.1016/j.micinf.2004.05.015.
16. S. J. Kopytek, J. C. Dyer, G. S. Knapp, J. C. Hu, Resistance to methotrexate due to AcrAB-dependent export from *Escherichia coli. Antimicrobial Agents and Chemotherapy* **44**, 3210-3212 (2000). https://doi.org/10.1128/aac.44.11.3210-3212.2000.
17. E. Gullberg *et al.*, Selection of Resistant Bacteria at Very Low Antibiotic Concentrations. *PLOS Pathogens* **7**, e1002158 (2011). https://doi.org/10.1371/journal.ppat.1002158.
18. E. Gullberg, L. M. Albrecht, C. Karlsson, L. Sandegren, D. I. Andersson, Selection of a Multidrug Resistance Plasmid by Sublethal Levels of Antibiotics and Heavy Metals. *mBio* **5**, e01918-01914 (2014). https://doi.org/10.1128/mBio.01918-14.
19. S. Westhoff *et al.*, The evolution of no-cost resistance at sub-MIC concentrations of streptomycin in *Streptomyces coelicolor*. *The ISME Journal* **11**, 1168-1178 (2017). https://doi.org/10.1038/ismej.2016.194.
20. N. L. Podnecky *et al.*, Conserved collateral antibiotic susceptibility networks in diverse clinical strains of *Escherichia coli*. *Nature Communications* **9**, 3673 (2018). https://doi.org/10.1038/s41467-018-06143-y.
21. M. C. Di Luca *et al.*, Low biological cost of carbapenemase-encoding plasmids following transfer from *Klebsiella pneumoniae* to *Escherichia coli. Journal of Antimicrobial Chemotherapy* **72**, 85-89 (2016). https://doi.org/10.1093/jac/dkw350.
22. Á. Nyerges *et al.*, A highly precise and portable genome engineering method allows comparison of mutational effects across bacterial species. *Proceedings of the National Academy of Sciences* **113**, 2502-2507 (2016). https://doi.org/10.1073/pnas.1520040113.
23. The European Committee on Antimicrobial Susceptibility Testing "Breakpoint tables for interpretation of MICs and zone diameters, Version 10.0," (EUCAST, 2020; http://www.eucast.org).
24. G. M. Eliopoulos, P. Huovinen, Resistance to Trimethoprim-Sulfamethoxazole. *Clinical Infectious Diseases* **32**, 1608-1614 (2001). https://doi.org/10.1086/320532.

25. P. Seideman, O. Beck, S. Eksborg, M. Wennberg, The pharmacokinetics of methotrexate and its 7-hydroxy metabolite in patients with rheumatoid arthritis. *British Journal of Clinical Pharmacology* **35**, 409-412 (1993). https://doi.org/10.1111/j.1365-2125.1993.tb04158.x.
26. E. S. Henderson, R. H. Adamson, V. T. Oliverio, The metabolic fate of tritiated methotrexate. II. Absorption and excretion in man. *Cancer Research* **25**, 1018-1024 (1965).
27. J. J. Sacco, J. Botten, F. Macbeth, A. Bagust, P. Clark, The Average Body Surface Area of Adult Cancer Patients in the UK: A Multicentre Retrospective Study. *PLOS ONE* **5**, e8933 (2010). https://doi.org/10.1371/journal.pone.0008933.
28. S. C. Howard, J. McCormick, C.-H. Pui, R. K. Buddington, R. D. Harvey, Preventing and Managing Toxicities of High-Dose Methotrexate. *Oncologist* **21**, 1471-1482 (2016). https://doi.org/10.1634/theoncologist.2015-0164.
29. H. Kruszewska, T. Zareba, S. Tyski, Antimicrobial activity of selected non-antibiotics - Activity of methotrexate against *Staphylococcus aureus strains*. *Acta Poloniae Pharmaceutica* **57 Suppl**, 117-119 (2000).
30. M. R. Moody *et al.*, Effect of Two Cancer Chemotherapeutic Agents on the Antibacterial Activity of Three Antimicrobial Agents. *Antimicrobial Agents and Chemotherapy* **14**, 737-742 (1978). https://doi.org/10.1128/aac.14.5.737.
31. A. Nyhlén, B. Ljungberg, I. Nilsson-Ehle, I. Odenholt, Bactericidal Effect of Combinations of Antibiotic and Antineoplastic Agents against *Staphylococcus aureus* and *Escherichia coli*. *Chemotherapy* **48**, 71-77 (2002). https://doi.org/10.1159/000057665.
32. Y. Wang *et al.*, Antiepileptic drug carbamazepine promotes horizontal transfer of plasmid-borne multi-antibiotic resistance genes within and across bacterial genera. *The ISME Journal* **13**, 509-522 (2019). https://doi.org/10.1038/s41396-018-0275-x.
33. J. N. Van der Beek *et al.*, The effect of leucovorin rescue therapy on methotrexate-induced oral mucositis in the treatment of paediatric ALL: A systematic review. *Critical Reviews in Oncology/Hematology* **142**, 1-8 (2019). https://doi.org/10.1016/j.critrevonc.2019.07.003.
34. Y. Wang *et al.*, Non-antibiotic pharmaceuticals enhance the transmission of exogenous antibiotic resistance genes through bacterial transformation. *The ISME Journal* **14**, 2179-2196 (2020). https://doi.org/10.1038/s41396-020-0679-2.
35. G. Kahlmeter, The ECO.SENS Project: a prospective, multinational, multicentre epidemiological survey of the prevalence and antimicrobial susceptibility of urinary tract pathogens--interim report. *The Journal of antimicrobial chemotherapy* **46 Suppl 1**, 15-22; discussion 63-15 (2000). https://doi.org/10.1093/jac/46.suppl_1.15.
36. H. Ikeda, J.-i. Tomizawa, Transducing fragments in generalized transduction by phage P1: I. Molecular origin of the fragments. *Journal of Molecular Biology* **14**, 85-109 (1965). https://doi.org/10.1016/S0022-2836(65)80232-7.
37. K. A. Datsenko, B. L. Wanner, One-step inactivation of chromosomal genes in *Escherichia coli* K-12 using PCR products. *Proceedings of the National Academy of Sciences* **97**, 6640 (2000). https://doi.org/10.1073/pnas.120163297.
38. D. Yu *et al.*, An efficient recombination system for chromosome engineering in *Escherichia coli*. *Proceedings of the National Academy of Sciences of the United States of America* **97**, 5978-5983 (2000). https://doi.org/10.1073/pnas.100127597.
39. S. K. Sharan, L. C. Thomason, S. G. Kuznetsov, D. L. Court, Recombineering: a homologous recombination-based method of genetic engineering. *Nature protocols* **4**, 206-223 (2009). https://doi.org/10.1038/nprot.2008.227.

40. J. Näsvall, A. Knöppel, D. I. Andersson, Duplication-Insertion Recombineering: a fast and scar-free method for efficient transfer of multiple mutations in bacteria. *Nucleic acids research* **45**, e33 (2017). https://doi.org/10.1093/nar/gkw1078.
41. Q. Tu *et al.*, Room temperature electrocompetent bacterial cells improve DNA transformation and recombineering efficiency. *Scientific Reports* **6**, 24648 (2016). https://doi.org/10.1038/srep24648.
42. L. M. Guzman, D. Belin, M. J. Carson, J. Beckwith, Tight regulation, modulation, and high-level expression by vectors containing the arabinose PBAD promoter. *Journal of Bacteriology* **177**, 4121-4130 (1995). https://doi.org/10.1128/jb.177.14.4121-4130.1995.
43. L. Imamovic *et al.*, Drug-Driven Phenotypic Convergence Supports Rational Treatment Strategies of Chronic Infections. *Cell* **172**, 121-134.e114 (2018). https://doi.org/10.1016/j.cell.2017.12.012.
44. L. Imamovic, M. O. A. Sommer, Use of Collateral Sensitivity Networks to Design Drug Cycling Protocols That Avoid Resistance Development. *Science Translational Medicine* **5**, 204ra132 (2013). https://doi.org/10.1126/scitranslmed.3006609.
45. R Core Team, "R: A language and environement for statistical computing. R Foundation for Statistical Computing", (The R Foundation, 2018; https://www.r-project.org).
46. M. Thulin, "BAT: an online tool for analysing growth curves", (2018; http://www.mansthulin.se/bat/).
47. D. E. Dykhuizen, Experimental Studies of Natural Selection in Bacteria. *Annual Review of Ecology and Systematics* **21**, 373-398 (1990). https://doi.org/10.1146/annurev.es.21.110190.002105.